06

Spectroscopy of diamond plates modified by electron beams

© A.A. Kostin, I.O. Podoilov, A.A. Kharlamova, A.A. Ladvishchenko, M.K. Eseev, D.N. Makarov, K.A. Makarova

Northern (Arctic) Federal University,
163002 Arkhangelsk, Russia
e-mail: a.kostin@narfu.ru; i.podojlov@narfu.ru; a.a.harlamova@narfu.ru; a.ladvischenko@narfu.ru; m.eseev@narfu.ru; makarovd0608@yandex.ru; k.makarova@narfu.ru

Received October 30, 2024
Revised October 30, 2024
Accepted October 30, 2024

Five monocrystalline type Ib plates with nitrogen nitrogen from 9 to 106 ppm, were irradiated with a dose of 10^{18} e/cm^2 electrons with an energy of 3 MeV and were annealed in vacuum at a temperature of 1200 °C during 24 hours. The dependence of the resonance signal magnitude on changes in the concentration of substitutive nitrogen as a result of electron irradiation and subsequent annealing was found by infrared spectroscopy and optically detectable magnetic resonance.

Keywords: diamond, defects, nitrogen vacancies, optically detectable magnetic resonance, infrared spectroscopy.

DOI: 10.61011/TP.2025.03.60851.366-24

Introduction

Optically active nitrogen-vacancy (NV) centers in diamond may assume negative (NV^-) or neutral (NV^0) charge states. NV^- centers have a number of unique properties and have various scientific and technical applications. NV^- centers are sensitive to magnetic fields; using optical instruments, one may read out the spin state and measure the coherence time. These properties are being studied actively at present [1–3]. Splitting of spin states of an NV^- center is observed under the influence of an external magnetic field. Such features of these centers are used for technical diagnostics (e.g., for measuring battery discharge currents [4]). The measurement of magnetic fields is used for non-destructive testing with a high degree of accuracy. The noncontact optically detected magnetic resonance (ODMR) method has been proven efficient in measurements of electromagnetic fields [5]. Magnetic field diagnostics also finds applications in medicine. Since the human body is diamagnetic in nature, magnetic diagnostics is effective in therapeutic use. Non-invasive methods of magnetic resonance imaging (MRI), hyperthermia and thermal ablation with magnetic nanoparticles, transcranial magnetic stimulation, etc., are known. The principle of non-maleficence is a key aspect of non-invasive diagnostics. The magnetic field gets weaker with distance from the source. This implies that in order to reach higher resolution and accuracy levels, one needs to devise diagnostic methods that provide an opportunity to shorten the distance to the source as much as possible without damaging the covering layer. A device capable of plotting a detailed map of magnetic fields may be a solution to this problem. Such a device requires a sensor that is sensitive to weak magnetic fields and may be brought close to the tissue [6]. Specifically, magnetoencephalography (MEG) allows for non-invasive diagnostics of the human brain. SQUID (superconducting quantum interference device) sensors are among the devices that may implement this method. Sensors of this type are based on the flow of tunnel currents, are highly sensitive to magnetic fields, and require a low temperature of approximately 4 K (the temperature of liquid helium) [7]. Liquid helium is quite expensive and requires complex storage and transfer setups; in addition, SQUID sensors cannot be brought close to living tissue without causing burns. An alternative to SQUID sensors capable of operating at room temperature is awaited. A sensor based on diamond with NV^- centers is a promising candidate in this context [8,9]. An NV pair and the ODMR method are used to record fluorescence that depends on the ground spin state of the NV^- center complex triplet. This state is controlled by an external magnetic field; the spin sublevels shift due to the Zeeman effect. Under the influence of gigahertz microwave radiation, the resonance peak, where the NV^- center complex luminescence excited by a laser at a wavelength of 532 nm decays resonantly, shifts in frequency in dependence to the magnetic field magnitude. The sensitivity of certain sensors has already reached a level of 344 pT/$\sqrt{\text{Hz}}$, which is well beyond the capabilities of conventional Hall sensors [10]. To integrate diamond plates with NV^- centers successfully into the hardware architecture, one needs to maintain a high signal-to-noise ratio for weak signal detection [11]. Certain systems reach a compromise by maintaining the optimum sensitivity at room temperature [12,13]. Calibration is performed to enhance the sensitivity of a diamond plate in a noisy environment (at room temperature). The coherence time is taken into account in this calibration, and the quantum mechanism is separated from statistical noise [14]. The construction of a quantum sensor necessitates diagnostics and calibration of the plate. It is hard to predict how the NV^- centers

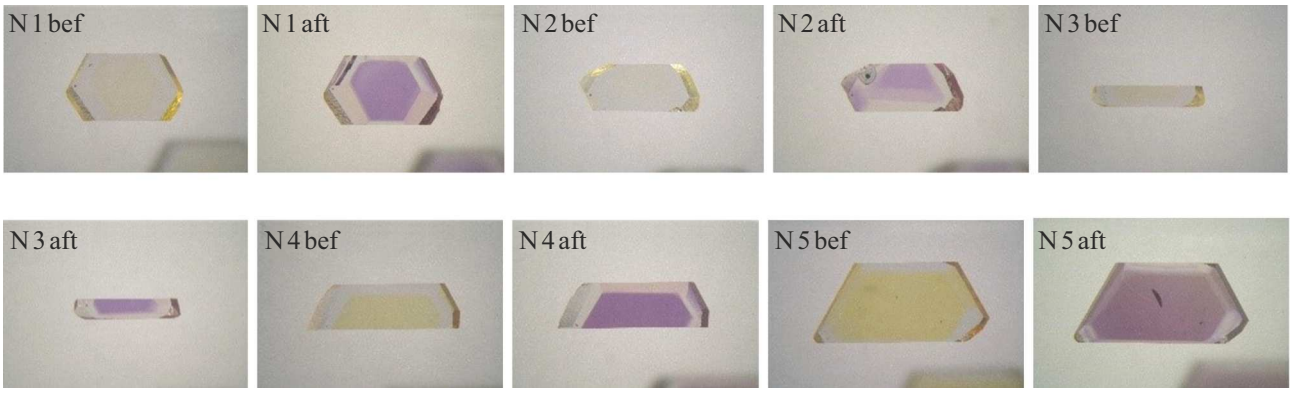

Figure 1. Diamond plates Nos. 1, 2, 3, 4, and 5 before (bef) and after (aft) irradiation with subsequent annealing in vacuum at a temperature of 1200 °C for 24 h. The initial nitrogen concentration increases with plate number. The concentration of single substitutional nitrogen atoms (C centers) before irradiation is 9, 17, 32, 51, and 106 ppm, respectively.

will align in the crystal lattice structure after all the growth and post-growth treatment procedures [15,16]. Electron irradiation of single-crystal nitrogen-doped diamond in an accelerator is the best known method for producing NV^- centers [17,18]. The formation of NV pairs and vacancies depends nonlinearly on the radiation dose and the initial nitrogen concentration [19,20]. To form a proper ensemble, one needs to set the optimum parameters providing a higher sensitivity. Other methods involve not only the selection of the initial parameters of a diamond plate and the characteristics of an applied electron beam, but also the production of diamond nanopillars with NV^- centers [21]. Having selected a set of plates, one may identify the general trends of ensemble formation using diagnostic methods. A universal diagnostic method allowing one to calculate the absolute concentration of NV^- centers, vacancies, and vacancy clusters in diamond is currently lacking [22,23]. The key parameters for fabrication of sensitive diamond sensors are a high concentration of NV^- centers throughout the plate volume and a combination of a long spin coherence time with a strong optical transition of NV^- centers [24]. Research is underway to optimize the intensity of high-energy electron irradiation with the aim of producing a sensitive diamond plate with NV^- centers. The efficiency of electron irradiation in raising the concentration of NV^- centers has been confirmed [25–27]. In the present study, we investigated diamond plates irradiated by a high-energy electron beam with subsequent annealing. IR spectroscopy [28] and ODMR were used to demonstrate a new method for estimating the concentration of NV^- centers.

1. Samples

Five single-crystal synthetic diamond plates grown in the Fe-Ni-C system by the HPHT (high pressure/high temperature) method at a temperature of approximately 1300 °C and a pressure of 50 kbar in a laboratory press-free ultra-high pressure BARS apparatus were selected. The crystals were type Ib; the nitrogen content varied from 9 to 106 ppm (yellow hue of varying intensity). The plate parameters were as follows: face length, no more than 6 mm; thickness, 0.5 mm with front face orientation {111}. Five plates were irradiated simultaneously by a linear electron accelerator with an irradiation dose of 10^{18} e/cm^2 and an energy of 3 MeV [29]. Following irradiation, the diamond plates were annealed in vacuum at a temperature of 1200 °C for 24 h (low pressure/high temperature (LPHT) annealing). Their color has changed. The resulting vacancies become mobile during annealing, forming NV^- centers with nitrogen and lending a violet hue to the plate. The samples imaged before and after irradiation with subsequent annealing are shown in Fig. 1.

2. Research methods

2.1. IR spectroscopy method

The methods of IR spectroscopy in the single-phonon region of the diamond spectrum in the mid-IR range reveal the primary nitrogen defects (C, C^+). The studied synthetic diamonds feature C centers (single substitutional nitrogen atoms) only; after irradiation, the same centers are also present in an ionized state (C^+ defects). An FT-801 IR Fourier spectrometer with a MICRAN-3 IR microscope produced by Simex (Novosibirsk) were used in transmission-mode measurements in the present study. IR absorption spectra were recorded at points located in a grid with a step of 95 μm. The light spot size (set by the aperture) was 100×100 μm. A mercury cadmium telluride (MCT) radiation receiver cooled with liquid nitrogen was used. The spectral resolution was 8 cm^{-1}. Four scans were performed at each point, and the results were averaged. The baseline spectrum was recorded in transmission without a sample in order to set a threshold against which the absorption intensity was measured after the passage of infrared radiation through

the sample. The spectra were recorded this way at each step, and a map of the distribution of IR absorption over the entire plate surface was plotted. All types of diamond are characterized by intrinsic IR absorption within the $4000-16000\,\mathrm{cm}^{-1}$ range where the absorption coefficients should correspond to the characteristic values. Each IR diamond plate spectrum was normalized by the intrinsic lattice absorption value of $(12.8 \pm 0.3)\,\mathrm{cm}^{-1}$ at 2170 and $2030\,\mathrm{cm}^{-1}$. The concentration formula was determined using the destructive method with subsequent combustion, wherein the nitrogen release was measured by capacitive manometry [30]. The concentration of C defects in diamond is related to absorption coefficient μ_{1130} at the $1130\,\mathrm{cm}^{-1}$ band in the following way:

$$\mathrm{N_C(ppm)} = (25 \pm 2) \cdot \mu_{1130}. \quad (1)$$

The absolute concentration value is determined by this formula. After irradiation, a fraction of C defects lose the fifth valence electron and are transformed into C^+ defects. The signal from C defects becomes weaker in this case, and the signal from C^+ defects emerges in the single-phonon region with the primary line at $1332\,\mathrm{cm}^{-1}$ [31].

2.2. ODMR method

The ODMR signal from the studied plates was recorded in the continuous mode in zero magnetic field. The ODMR diagram is shown in Fig. 2.

Optical excitation was provided by a Cobolt Samba semiconductor laser with a wavelength of 532 nm. An optical slit was used to isolate the most intense beam of the first diffraction order. The first-order beam then passed through a neutral filter (NF) and was reflected off the DMLP550 series dichroic mirrors. Fed through an MY5X-802-5X objective, the laser beam incident on the diamond plate formed a spot with an approximate diameter of $100\,\mu$m. Emission excited by this laser was focused through a long-wave filter (LWF) of the FEL0550 series onto an APDC12703 photodetector (PhD). Microwave radiation was supplied by a flat antenna with a diameter of 1 mm in the form of a printed circuit board positioned

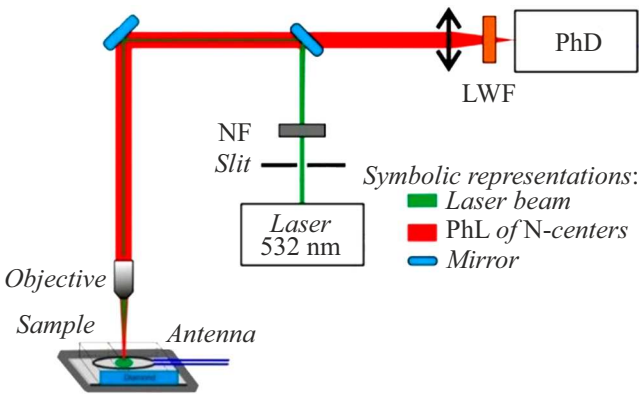

Figure 2. ODMR diagram.

right under the sample [32]. The laser power exciting room-temperature luminescence of NV^- centers did not vary in the process of irradiation of the samples. The diamond plate was mapped using a motorized stage with a pitch of 100 *mu*m.

3. Results and discussion

Let us assume that the luminescence intensity at the resonant frequency will decrease in proportion to the concentration of negatively charged NV^- centers. An ensemble of NV^- centers is excited under laser irradiation, and the luminescence intensifies with an increase in the concentration of the ensemble. Applying microwave radiation to the diamond plate, we suppress the ensemble luminescence. Note that the magnitude of signal reduction depends on a number of parameters. The intensity of luminescence of an NV^- center depends on temperature [33], and the change in luminescence of a plate with NV^- centers at the resonant frequency depends on the spatial inhomogeneity of microwave radiation [34]. With refraction and diffraction taken into account, the luminescence signal is scattered in different directions in the diamond plate, and this limits the fraction of signal intensity that reaches the photodetector [35]. These factors are less significant in our measurements due to the variation of the initial nitrogen concentration. The difference in average concentration of C defects in low-nitrogen diamond plates is 8 ppm; in diamond plates with a high nitrogen content, the difference in average concentration of C defects is 20 ppm or more. As a result of electron irradiation with subsequent annealing, a certain fraction of nitrogen passes into optically active NV^- centers (also with different concentration). This concentration may be estimated from the difference in luminescence signals of different diamond plates. The reduction in luminescence of an ensemble of NV^- centers at the resonant frequency of microwave radiation should become more profound at their higher concentration. To substantiate this assumption, one needs to analyze the dependence of luminescence difference ΔU (μV) on the ratio of concentrations of C defects before irradiation and after irradiation with subsequent annealing — $(\mathrm{N_C})_{bef}/(\mathrm{N_C})_{aft}$.

Figure 3 presents the normalized IR spectrum obtained before and after irradiation with electrons at a dose of $10^{18}\,\mathrm{e/cm}^2$ and an energy of 3 MeV with subsequent annealing.

This IR spectrum of one of the samples was recorded in the $100 \times 100\,\mu$m region to illustrate the bands where the radiation intensity is absorbed. All of the studied samples are characterized by similar spectra. The differences between them are limited mostly to the absorption intensity.

The absorption bands were determined from the IR spectrum. Each sample is characterized by the following. Absorption at the $1130\,\mathrm{cm}^{-1}$ band (C defect) is observed prior to irradiation with subsequent annealing. After irradiation followed by annealing, this absorption at the

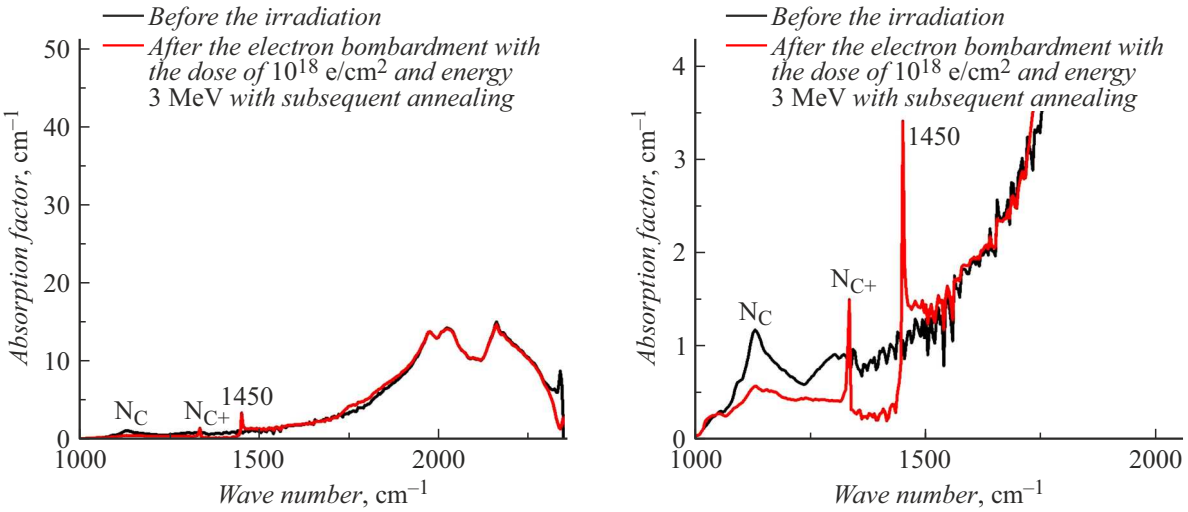

Figure 3. Left — IR absorption spectrum of a type Ib plate before and after electron irradiation at a dose of 10^{18} e/cm^2 and an energy of 3 MeV with subsequent annealing. Right — the same, but the ordinate axis scale is smaller.

1130 cm^{-1} band gets suppressed, and the formation of positively charged nitrogen in the substitutional position at the 1332 cm^{-1} band is observed. A peak at the 1450 cm^{-1} band, which is associated with the formation of an H1a defect (an isolated nitrogen atom in an interstitial position), is also well-pronounced [36].

In view of the segmental distribution, the calculation of the average concentration of newly formed defects throughout the entire plate volume will not be reliable. The concentration of C defects decreased due to their transformation into other types of defects in the process of annealing. Therefore, the average concentration of C defects before and after irradiation with subsequent annealing $((N_C)_{bef}/(N_C)_{aft})$ was calculated. The values of average concentration $(N_C)_{bef}$ (ppm) of C defects before irradiation, average concentration $(N_C)_{aft}$ (ppm) of C defects after irradiation with subsequent annealing, and ratio $(N_C)_{bef}/(N_C)_{aft}$ for each diamond plate are listed in the table.

The ODMR signal is shown in Fig. 4.

ODMR was used just to record the average value of luminescence difference from the diamond plate at a resonant frequency of 2866 MHz. The total luminescence signal within the entire spectral optical range was not measured, since NV^- center luminescence was of interest to us. Other complexes in the diamond plate produce luminescence at other frequencies, but it may be regarded as noise. Noise could be related to the process of photoionization of NV^- into NV^0 [37]. The average ΔU (μV) values are presented in the table.

Figure 5 shows the dependence of averaged luminescence value ΔU on ratio $(N_C)_{bef}/(N_C)_{aft}$ of the averaged concentrations of C defects before irradiation and after irradiation with subsequent annealing.

The dependence for samples with a low nitrogen content (samples Nos. 1 and 2) appears to be consistent with the

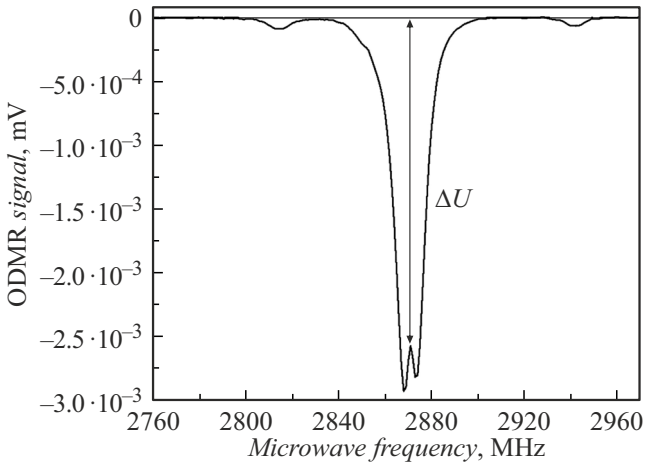

Figure 4. ODMR signal.

hypothesis described above. A larger amount of nitrogen in C defects aggregated with single vacancies, and luminescence difference ΔU at a resonant frequency of 2866 MHz increases at a higher value of ratio $(N_C)_{bef}/(N_C)_{aft}$. The analysis for samples with a higher nitrogen content (samples Nos. 3, 4, and 5) becomes more complex, and nonlinearity is observed. One should keep in mind that, as was indicated above, C defects and optically active NV^- centers were joined by other defects that emerged in diamond in the process of annealing. Vacancies and interstitial atoms are formed after irradiation. In addition to negatively charged NV^- centers, neutral NV^0 centers form during annealing. Neutral NV^0 centers are optically active centers with photoluminescence at a wavelength of 575 nm. The sensitivity of the photodetector at a wavelength of 637 nm (photoluminescence of a negatively charged NV^- center) is approximately 10 times greater than its sensitivity

Average concentration of C defects and ODMR maps of diamond plates

Sample	ODMR map. The scale represents receiver signal intensity with variation ΔU, mV	$(N_C)_{bef}$, ppm	$(N_C)_{aft}$, ppm	$(N_C)_{bef}/(N_C)_{aft}$	Average value ΔU, μV
№ 1		9	2	4.5	2.4
№ 2		17	11	1.5	1.2
№ 3		32	26	1.23	2.1
№ 4		51	48	1.06	3.3
№ 5		106	87	1.2	2.4

at 575 nm (photoluminescence of a neutral NV^0 center). The formation of NV^- centers is grossly predominant at high concentrations of donor nitrogen (above 3.5 ppm) [38]. Samples with a donor nitrogen concentration of 9 ppm and higher are considered in the present study. In view of the above, the influence of NV0 centers on the ODMR signal may be neglected. Nitrogen interstitials (an isolated nitrogen atom in an interstitial position) are formed as a result of annealing of irradiated diamond plates. Irradiation induces the formation of intrinsic interstitials that move along the crystal in the course of annealing and drive nitrogen atoms into interstitial positions. The conversion of C defects into NV^- centers was only partial in samples Nos. 3 and 5. A C defect could lose its fifth valence electron and enter a C^+ state. Sample No. 3 requires further analysis. If we consider the possibility that vacancy clusters unable to drift within the crystal lattice volume during annealing form at a high irradiation dose, this statement is not entirely accurate, since

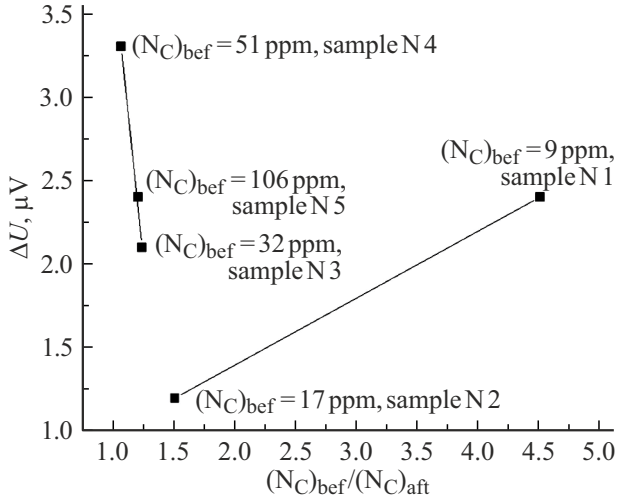

Figure 5. Dependence of luminescence difference ΔU (μV) on the ratio of concentrations of C defects before irradiation and after irradiation with subsequent annealing $(N_C)_{bef}/(N_C)_{aft}$.

vacancies are annealed completely in 24 h of heat treatment at 1200 °C [39]. The concentration of C defects in sample No. 5 is higher than 100 ppm; it is likely that nitrogen coagulates interfered with the formation of optically active defects [40]. The luminescence of sample No. 4 decreases more profoundly than in other samples; therefore, it has the highest concentration of NV^- centers. Analyzing the extreme values (samples Nos. 1 and 4), we find that the conversion of C defects into NV^- centers in low-nitrogen plate No. 1 is the highest. A tentative boundary at which the greatest number of C defects is converted into NV^- centers may be traced. A high concentration of NV^- centers is produced in sample No. 4 with initial concentration of C defects $(N_C)_{bef} \approx 50$ ppm after electron irradiation at a dose of 10^{18} e/cm^2 and an energy of 3 MeV with subsequent annealing at a temperature of 1200 °C for 24 h.

Conclusion

The mechanism of formation of NV^- centers in five single-crystal diamond plates with different nitrogen concentrations irradiated with electrons at a dose of 10^{18} e/cm^2 and an energy of 3 MeV with subsequent annealing in vacuum at a temperature of 1200 °C for 24 h was examined. The crystal was type Ib, and the orientation of front faces of plates was {111}. IR spectroscopy and ODMR methods were used. The dependence of ODMR luminescence difference on the ratio of concentrations of C defects before irradiation and after irradiation with subsequent annealing was plotted. A relation between the reduction in concentration of C defects and the conversion (as a result of post-growth engineering) of a nitrogen atom and a vacancy into an NV^- center was revealed.

The following conclusions may be made:

The highest conversion of C defects into NV^- centers is observed in the low-nitrogen plate.

The sample with a single nitrogen (C defect) concentration of ≈ 50 ppm had the strongest ODMR signal, indicating a high conversion of C defects into NV^- centers.

Further studies by positron annihilation spectroscopy (PAS) are required. The PAS method may be used to determine the influence of vacancy clusters on the formation of NV^- centers.

Funding

This study was supported by the Russian Science Foundation (grant No. 23-12-20014, https://rscf.ru/project/23-12-20014/) and the Ministry of Education and Science of the Russian Federation under state assignment FSRU-2024-0005 as part of the research work of the laboratory for diagnostics of carbon materials and spin-optical properties of wide-gap semiconductors.

Conflict of interest

The authors declare that they have no conflict of interest.

References

[1] F. Gorrini, A. Bifone. Biosensors, **13**, 691 (2023). DOI: 10.3390/ bios13070691
[2] A. Shames, A. Panich, L. Friedlander, H. Cohen, J. Butler, R. Moreh. Materials, **17**, 1871 (2024). DOI: 10.3390/ma17081871
[3] Q. Liu, Z. Lan, W. Guo, J. Deng, X. Peng, M. Chi, S. Li. Sensors, **24**, 5532 (2024). DOI: 10.3390/s24175532
[4] Yu. Hatano, J. Shin, J. Tanigawa, Yu. Shigenobu, A. Nakazono, T. Sekiguchi, Sh. Onoda, T. Ohshima, K. Arai, T. Iwasaki, M. Hatano. Sci. Reports, **12**, Art. Num. 13991 (2022).
[5] Yi. Hu, G.Z. Iwata, L. Bougas, J.W. Blanchard, A. Wickenbrock, G. Jakob, S. Schwarz, C. Schwarzinger, A. Jerschow, D. Budker. Appl. Sci., **10**, 7864 (2020). DOI: 10.3390/app10217864
[6] S. Rotundo, D. Brizi, A. Flori, G. Giovannetti, L. Menichetti, A. Monorchio. Sensors, **22**, 5132 (2022). DOI: 10.3390/s22145132
[7] Y. Feng, W. Xiao, T. Wu, J. Zhang, J. Xiang, H. Guo. Appl. Sci., **11**, 2415 (2021). DOI: 10.3390/ app11052415
[8] G. Chen, W. Wang, F. Lin, M. Zhang, Q. Wei, C. Yu, H.-X. Wang. Materials, **15**, 2557 (2022). DOI: 10.3390/ma15072
[9] A. Crnjac, N. Skukan, G. Provatas, M. Rodriguez-Ramos, M. Pomorski. Materials, **13**, 2473 (2020).
[10] F.M. Stürner, A. Brenneis, T. Buck, J. Kassel, R. Rölver, T. Fuchs, A. Savitsky, D. Suter, J. Grimmel, S. Hengesbach, M. Fortsch, K. Nakamura, H. Sumiya, Sh. Onoda, Ju. Isoya, F. Jelezko. Adv. Quant. Technol., **4**, 2000111 (2021).
[11] V.M. Acosta, E. Bauch, M.P. Ledbetter, C. Santori, K.M.C. Fu, P.E. Barclay, R.G. Beausoleil, H. Linget, J.F. Roch, F. Treussart, S. Chemerisov, W. Gawlik, D. Budker. Phys. Rev. B, **80**, 115202 (2009).

[12] P.C.D. Hobbs. *Building Electro-Optical Systems: Making It All Work*, 3rd ed. Wiley *Series in Pure and Applied Optics* (John Wiley & Sons Inc., Hoboken, NJ., USA, 2022)
[13] V.K. Sewani, H.H. Vallabhapurapu, Ya. Yang, H.R. Firgau, Ch. Adambukulam, B.C. Johnson, J.J. Pla, A. Laucht. American J. Phys., **88**, 1156 (2020). DOI: 10.1119/10.0001905
[14] R.A. Babunts, A.S. Gurin, Yu.A. Uspenskaya, K.V. Likhachev, V.V. Yakovleva, A.V. Batueva, A.M. Skomorokhov, I.P. Veyshtort, M.V. Uchaev, M.K. Eseev, V.G. Vins, A.P. Yelisseyev, Z.F. Urmantseva, P.G. Baranov. Appl. Magn. Resonance, **55** (4), 417 (2024).
[15] D. Makarov, M. Eseev, E. Gusarevich, V. Matveev, K. Makarova, M. Borisov. Crystals, **14** (2), 193 (2024).
[16] M. Eseev, K. Makarova, D. Makarov. Crystals, **12** (10), 1417 (2022).
[17] B. Campbell, A. Mainwood. Phys. Status Solidi Appl. Res., **181**, 99 (2000).
[18] J.G. Seo, Y.K. Ahn, J.W. Park. Met. Mater. Int., **17**, 1031 (2011).
[19] I.N. Meshkov, M.K. Eseev, I.V. Kuziv, A.A. Kostin, A.A. Sidorin, O.S. Orlov. Phys. Part. Nuclei Lett., **20**, 757 (2023). DOI: 10.1134/S1547477123040507
[20] I.N. Meshkov, M.K. Eseev, I.V. Kuziv, A.A. Kostin, A.A. Sidorin, O.S. Orlov. Phys. Part. Nuclei Lett., **20** (4), 757 (2023).
[21] K. Volkova, Ju. Heupel, S. Trofimov, F. Betz, R. Colom, R.W. MacQueen, S. Akhundzada, M. Reginka, A. Ehresmann, J.P. Reithmaier, S. Burger, C. Popov, B. Naydenov. Nanomaterials, **12**, 1516 (2022). DOI: 10.3390/nano12091516
[22] I.N. Meshkov, M.K. Eseev, I.V. Kuziv, A.A. Kostin, A.A. Sidorin, O.S. Orlov. Phys. Part. Nuclei Lett., **21**, 526 (2024). DOI: 10.1134/S1547477124700523
[23] M.K. Eseev, I.V. Kuziv, A.A. Kostin, I.N. Meshkov, A.A. Sidorin, O.S. Orlov. Materials, **16** (1), 203 (2023).
[24] T. Luo, L. Lindner, J. Langer, V. Cimalla, X. Vidal, F. Hahl, C. Schreyvogel, S. Onoda, S. Ishii, T. Ohshima, D. Wang, D.A. Simpson, B.C. Johnson, M. Capelli, R. Blinder, J. Jeske. New J. Phys., **24**, 033030 (2022).
[25] S.C. Benjamin, B.W. Lovett, J.M. Smith. Las. Phot. Rev., **3**, 556 (2009).
[26] S. Ishii, S. Saiki, S. Onoda, Y. Masuyama, H. Abe, T. Ohshima. Quantum Beam Sci., **6**, 2 (2022). DOI: 10.3390/qubs6010002
[27] A.M. Gorbachev, M.A. Lobaev, D.B. Radishchev, A.L. Vikharev, S.A. Bogdanov, M.N. Drozdov, V.A. Isaev, S.A. Kraev, A.I. Okhapkin, E.A. Arkhipova. Radiophys. Quant. Electron., **63** (7), (2020).
[28] A.M. Zaitsev. *Optical Properties of Diamond: A Data Handbook* (Springer, Berlin, 2001)
[29] S.I. Molokovskii, A.D. Sushkov. *Intensivnye elektronnye i ionnye puchki* (Energoatomizdat, M., 1991) (in Russian).
[30] S.R. Boyd, I. Kiflawi, G.S. Woods. Phil. Mag. B, **69**, 1149 (1994).
[31] S.C. Lawson, D. Fisher, D.C. Hunt, M.E. Newton. J. Phys. Condens. Matter, **10**, 6171 (1998).
[32] K. Sasaki, Ya. Monnai, S. Saijo, R. Fujita, H. Watanabe, J. Ishi-Hayase, K.M. Itoh, E. Abe. Rev. Sci. Instrum., **87**, 053904 (2016).
[33] G. Kucsko, P.C. Maurer, N.Y. Yao, M. Kubo, H.J. Noh, P.K. Lo, H. Park, M.D. Lukin. Nature, **500**, 54 (2013).
[34] O.R. Opaluch, N. Oshnik, R. Nelz, E. Neu. Nanomaterials, **11**, 2108 (2021). DOI: 10.3390/ nano11082108
[35] F. Jelezko, J. Wrachtrup. Phys. Stat. Sol. (a), **20**, 3207 (2006).
[36] I. Kiflawi, G. Davies, D. Fisher, H. Kanda. Diamond Relat. Mater, **8**, 1576 (1999).
[37] C.E. Avalos. *Detection and Polarization of Nuclear and Electron Spins using Nitrogen-Vacancy Centers: Doctoral Thesises* (University of California, Berkeley, 2014)
[38] A.T. Collins, A. Connor, Ch.-H. Ly, A. Shareef. P.M. Spear. J. Appl. Phys., **97**, 083517 (2005). DOI: 10.1063/1.1866501
[39] G. Davies, A.T. Collins. Diamond Relat. Mater., **8**, 1847 (1993).
[40] A. Setzer, P.D. Esquinazi, O. Daikos, T. Scherzer, A. Pöppl, R. Staacke, T. Lühmann, S. Pessagna, W. Knolle, S. Buga, B. Abel, J. Meijer. Phys. Status Solidi B, **258**, 2100395 (2021). DOI: 10.1002/pssb.202100395

Translated by D.Safin